Microb Ecol
DOI 10.1007/s00248-016-0739-3

ENVIRONMENTAL MICROBIOLOGY

Artificial Intelligence for the Evaluation of Operational Parameters Influencing Nitrification and Nitrifiers in an Activated Sludge Process

Oluyemi Olatunji Awolusi[1] · **Mahmoud Nasr**[1] · **Sheena Kumari**[1] · **Faizal Bux**[1]

Received: 31 August 2015 / Accepted: 8 February 2016

Abstract Nitrification at a full-scale activated sludge plant treating municipal wastewater was monitored over a period of 237 days. A combination of fluorescent in situ hybridization (FISH) and quantitative real-time polymerase chain reaction (qPCR) were used for identifying and quantifying the dominant nitrifiers in the plant. Adaptive neuro-fuzzy inference system (ANFIS), Pearson's correlation coefficient, and quadratic models were employed in evaluating the plant operational conditions that influence the nitrification performance. The ammonia-oxidizing bacteria (AOB) abundance was within the range of 1.55×10^8–1.65×10^{10} copies L^{-1}, while *Nitrobacter* spp. and *Nitrospira* spp. were 9.32×10^9–1.40×10^{11} copies L^{-1} and 2.39×10^9–3.76×10^{10} copies L^{-1}, respectively. Specific nitrification rate (q_N) was significantly affected by temperature (r 0.726, p 0.002), hydraulic retention time (HRT) (r −0.651, p 0.009), and ammonia loading rate (ALR) (r 0.571, p 0.026). Additionally, AOB was considerably influenced by HRT (r −0.741, p 0.002) and temperature (r 0.517, p 0.048), while HRT negatively impacted *Nitrospira* spp. (r −0.627, p 0.012). A quadratic combination of HRT and food-to-microorganism (F/M) ratio also impacted q_N (r^2 0.50), AOB (r^2 0.61), and *Nitrospira* spp. (r^2 0.72), while *Nitrobacter* spp. was considerably influenced by a polynomial function of F/M ratio and temperature (r^2 0.49). The study demonstrated that ANFIS could be used as a tool to describe the factors influencing nitrification process at full-scale wastewater treatment plants.

Keywords Adaptive neuro-fuzzy inference system · Ammonia-oxidizing bacteria · Nitrite-oxidizing bacteria · Operational parameters · Statistical tools

Introduction

Ammonia toxicity is one of the several forms of nitrogen pollution that exist in aquatic environments [1]. Ammonia can be harmful to aquatic life and contributes to eutrophication of water bodies [2]. Moreover, at sufficiently high levels, ammonia can create a large oxygen demand in receiving waters, where the total consumption of oxygen is 4.57 g O_2 g^{-1} N-NH_4^+ oxidized [3]. In this context, ammonia removal from wastewater is one of the primary tasks to protect water resources from pollution discharges. Biological nitrification-denitrification is the most commonly used process for removing nitrogen from wastewater [4]. During nitrification process, ammonia (NH_3) is converted to nitrite (NO_2^-) by ammonia-oxidizing bacteria (AOB), while nitrite-oxidizing bacteria (NOB) convert the NO_2^- to nitrate (NO_3^-) [5]. In denitrification, NO_3^- is reduced to nitrogen gas (N_2) in a four-step process, in which NO_2^-, nitric oxide (NO), and nitrous oxide (N_2O) are electron acceptors in energy generating reactions [6].

Nitrifying bacteria are highly sensitive to changes in environmental parameters and plant operational conditions, such as pH, temperature, dissolved oxygen (DO) level, organic loading rate (OLR), ammonia loading rate (ALR), and hydraulic retention time (HRT) [7]. Neutral to slightly basic pH range (7.5 to 8.5) has been reported as optimum for efficient nitrification [8]. According to an earlier finding, at neutral pH,

Electronic supplementary material The online version of this article (doi:10.1007/s00248-016-0739-3) contains supplementary material, which is available to authorized users.

✉ Faizal Bux
faizalb@dut.ac.za

[1] Institute for Water and Wastewater Technology, Durban University of Technology, Durban 4000, South Africa

Published online: 23 February 2016

99 % of ammonia was removed. However, this dropped to about 75 % at a basic pH of 9.7 while acidic pH (4.8) resulted in an impaired removal efficiency of 56 % [7]. Although it was reported that nitrification would proceed at a temperature range of 20 to 37 °C [9], nonetheless niche differentiation exists among the members of NOB group with *Nitrobacter* having preference for relatively low temperatures (24–25 °C) while *Nitrospira* thrives at higher temperatures of 29–30 °C [10]. Kim et al. [1] demonstrated that raising temperature from 20 to 30 °C resulted in a 5.3-fold increase in ammonia oxidation and a 2.6-fold increase in nitrite oxidation. Lower nitrification performance has been observed at higher organic loading due to the competition for DO between heterotrophic bacteria and autotrophic nitrifying organisms in wastewater treatment system, [11]. Huang et al. [10] demonstrated that higher DO concentrations were more suitable to *Nitrobacter* growth, while *Nitrospira* were selectively enriched when DO concentrations were less than 1.0 mg/L. The available carbon substrate for the unit mass of microorganism (known as F/M ratio) can also impact nitrification. A study by Wu et al. [11] suggested that high F/M ratio should be avoided to minimize its negative impact on nitrification, and it indicated that F/M ratio between 0.2 and 0.4 was the optimum range for nitrification. The influence of HRT on nitrification efficiency was also observed when HRT decreased from 30 to 5 h with a resultant increase in specific ammonium-oxidizing and nitrate-forming rates [12]. Additionally, the decrease in HRT led to a reduction of AOB population density, whereas the NOB, especially the fast growing *Nitrobacter* spp., increased significantly [12].

Modeling of a full-scale wastewater treatment plant (WWTP), operated under an uncontrolled environment, requires advanced nonlinear modeling tools to simulate the complex relationships between inputs and outputs [1]. According to Klemetti [13], due to simultaneous dependence on different factors, competition between microbial groups is usually nonlinear. Artificial intelligence (AI) is an example of a nonlinear system that is capable of depicting the interactive influence between variables as well as their correlation with the simulation output [14]. AI incorporates artificial neural network (ANN), fuzzy inference system (FIS), and adaptive-neuro fuzzy inference system (ANFIS). ANN has the ability to model nonlinear systems efficiently owing to their high accuracy, adequacy, and quite promising applications in engineering [15]. FIS allows a logical data-driven modeling approach, which uses "if–then" rules and logical operators to establish qualitative relationships among the variables [16]. ANFIS is a neuro-fuzzy system that has the potential to capture the benefits of both ANN and FIS in a single framework [14]. Moreover, ANFIS can handle complex and highly nonlinear relationships between several parameters, without the difficult task of dealing with deterministic nonlinear mathematics [17]. Modeling based on ANFIS needs a little knowledge about the process to track given input/output data. In this context, it is expected that the effect of system operation on nitrification process could be studied using ANFIS. To the best of our knowledge, this is the first study applying ANFIS technique to describe the nitrification performance at a real WWTP subjected to dynamic operational parameters.

In this study, fluorescent in situ hybridization (FISH) and quantitative real-time polymerase chain reaction (qPCR) were used for detecting and quantifying the dominant nitrifiers at a full-scale WWTP. The effect of operational parameters and environmental conditions on nitrification was also investigated. An ANFIS was applied to select and rank the operational conditions that mostly influence the nitrification process. ANFIS results were further validated with cross-correlation coefficients and quadratic models.

Materials and Methods

Plant Description

The full-scale WWTP under study is situated in the Midlands of KwaZulu-Natal province, South Africa. The plant receives a discharge of $82{,}880 \pm 20{,}832\ m^3\ day^{-1}$ (average dry weather flow), including 90 % domestic and 10 % industrial wastewaters. The plant was designed based on the criteria of a Johannesburg configuration, which allow for nitrification/denitrification biological process [18]. As shown in Fig. 1, the effluent from primary settling tank is distributed to the pre-anoxic and anaerobic tanks. The pre-anoxic basin is further enriched with return activated sludge from the bottom of a final settler. The effluent from anaerobic tank is discharged into the anoxic unit. An internal recycle is pumped from the last part of aerobic units to the anoxic zone. The mixed liquor, containing activated sludge, flows from the aerobic zone to a secondary settler, where it is separated under a quiescent condition into treated wastewater and return activated sludge.

Sampling Protocol

The WWTP was monitored for a period of 237 days, i.e., from May to July 2012 and from November 2012 to March 2013. The study period was divided into two phases. Phase 1 represents the winter period during the first 78th days; and phase 2, the summer season from the 79th to the 237th day. Composite sludge samples, from the aerobic chamber, in addition to influent and effluent wastewater samples were collected twice per month. All samples were kept on ice while in transit to the lab.

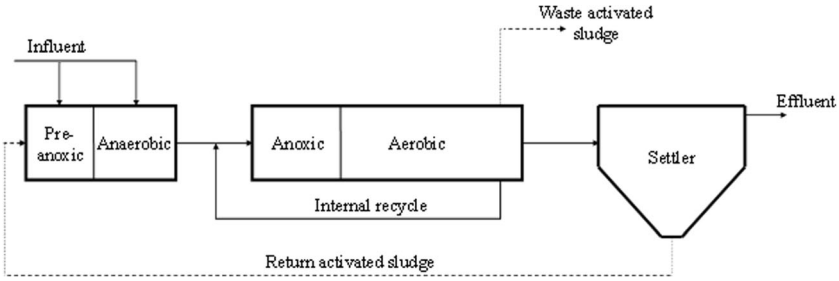

Fig. 1 Schematic diagram of the full-scale biological treatment process under study

Fluorescent In Situ Hybridization

FISH analysis was performed for initial identification of the nitrifying community according to the Fuchs et al. [19] protocol with modification. Sample preparation, immobilization on glass slides, dehydration, permeabilization, quality check of probes, and hybridization were undertaken as described earlier by Nielsen [20]. The samples were sonicated at 8 W for 10 min to disperse the flocs before performing the hybridization. Oligonucleotide probes targeting betaproteobacterial AOB and genus *Nitrobacter* spp. and *Nitrospira* spp., namely, Nso1225 [21], NIT3 [22], and Ntspa662 [12], respectively, were used (Table 1). The probes were labeled with CAL Fluor Red 590 fluorescence dye (Inqaba Biotechnical Industry (Pty), South Africa). The samples were visualized using a Zeiss AxioCam HRm (Carl Zeiss, Germany) epifluorescent microscope. Image analysis was carried out using a Zeiss AxioVision Release 4.6 (12-2006) imaging software.

DNA Extraction and Real-Time Quantitative PCR Amplification

Genomic DNA was extracted from sludge samples according to the Purkhold et al. [23] procedure. Quality and quantity of the extracted DNA were ascertained with a NanoDrop ND-1000 spectrophotometer (NanoDrop Technologies, USA). Individual standard curves were prepared for the different nitrifiers using purified 16S rRNA gene fragments (target DNA) obtained from PCR-amplified AOB (amoA-1F and amoA-2R), *Nitrobacter* spp. (FGPS872f and FGPS1269r), and *Nitrospira* spp. (NSR1113F and NSR1264R) as described by [24, 25] (Table 2). The concentrations were used in calculating their copy by considering their molecular weight and Avogadro's number. For qPCR standard curves, 10-fold serial dilutions of the target DNA were prepared from 10^8 to 10^1 copy numbers. The real-time PCR quantification was carried out according to modification of the method described by Steinberg and Regan [26] using Bio-Rad C1000 Touch Thermal Cycler-CFX96 Real-Time System (Bio-Rad, USA). For the quantitative real-time PCR, the primers already described in Table 2 were used. The optimized protocols used for quantifying the nitrifiers are shown in Table 3. To confirm amplification of the correct product, the amplicons from qPCR were electrophoresed in 1.2 % (*w*/*v*) agarose gel for the presence of the expected gene product sizes. The qPCR standard curve parameters used for the analysis are listed in Table 4.

Analytical Analysis

Concentrations of inorganic nitrogen species and chemical oxygen demand (COD) were estimated using standard methods [27]. Temperature, DO, and pH measurements were carried out using the YSI 556 MPS (Multiprobe System).

Calculations

Operational conditions such as HRT, OLR, ALR, and F/M ratio were calculated as mentioned in Tchobanoglous et al. [28] as follows (Eqs. 1, 2, 3, and 4):

$$HRT = \frac{V}{Q} \tag{1}$$

$$OLR = \frac{Q \times COD}{V} \tag{2}$$

$$ALR = \frac{Q \times N{-}NH_4{}^{+}}{V} \tag{3}$$

$$F/M = \frac{Q \times COD}{MLSS \times V} \tag{4}$$

Table 1 rRNA—targeted oligonucleotide probes and their specificity

Probe name	Target	Sequence (5′–3′)	FA (%)	Reference
NSO 1225	Betaproteobacterial AOB	CGCCATTGTATTACGTGTGA	35	[21]
NIT3	Genus *Nitrobacter*	CCTGTGCTCCATGCTCCG	40	[22]
Ntspa 662	Genus *Nitrospira*	GGAATTCCGCGCTCCTCT	35	[12]

FA formamide

Table 2 List of primers used and the optimized annealing temperature

Target	Primer	Annealing (°C)	References
AOB amoA	amoA-1F/amoA-2R	55	[25]
Nitrobacter 16S rDNA	FGPS872/FGPS1269	50	
Nitrospira 16S rDNA	NSR1113F/NSR1264R	65	

where *HRT* is the hydraulic retention time; *V* is the reactor volume; *Q* is the flow rate; *OLR* is the organic loading rate; *COD* is the chemical oxygen demand; *ALR* is the ammonia loading rate; *N-*NH_4^+ is the ammonia nitrogen; *F/M* ratio is the food-to-microorganisms ratio; and MLSS is the mixed liquor suspended solids.

Adaptive Neuro-Fuzzy Inference System

Architecture of ANFIS

To present the ANFIS architecture, two fuzzy if–then rules based on a first-order Takagi–Sugeno fuzzy model were considered:

Rule-1: If (x is A_1) and (y is B_1), then ($f_1 = p_1x + q_1y + r_1$)
Rule-2: If (x is A_2) and (y is B_2), then ($f_2 = p_2x + q_2y + r_2$)

where x and y are the inputs; A_1 and B_1 are the fuzzy sets; f_1 is the outputs within the fuzzy region specified by the fuzzy rule; and p_1, q_1 and r_1 are the design parameters determined during the training process.

As shown in Fig. 2, the ANFIS architecture to implement these two rules has a total of five layers, in which a circle indicates a fixed node, whereas a square indicates an adaptive node. The functioning of each layer can be described as follows [29]

Layer-1 (input node): Parameters in this layer are referred to "premise parameters." Every single node generates a fuzzy membership grade of linguistic label. The membership functions (MFs) of A_i and B_{i-2} are given by Eqs. 5 and 6, respectively:

$$O_i^1 = \mu_{A_i}(x) \quad i = 1, 2 \tag{5}$$

$$O_i^1 = \mu_{B_{i-2}}(y) \quad i = 3, 4 \tag{6}$$

where x (or y) is the input to node i and A_i (or B_{i-2}) is the linguistic label (small, large, etc.) related to this node. If the bell-shaped MF is generalized, $\mu_{A_i}(x)$ is given by Eq. 7:

$$\mu_{A_i}(x) = \frac{1}{1 + \left\{ \left(\frac{x - c_i}{a_i} \right)^2 \right\}^{b_i}} \tag{7}$$

where a_i, b_i, and c_i are the MF parameters, governing the bell-shaped functions accordingly.

Layer-2 (rule nodes): In the second layer, the nodes are labeled with *M*, indicating that they perform as a simple multiplier. The AND/OR operator is used to get one output that represents the antecedent of the fuzzy if–then rule. The outputs of this layer are defined as firing strengths of the rules. Each node analyzes the firing strength by cross multiplying all the incoming signals (Eq. 8):

$$O_i^2 = w_i = \mu_{A_i}(x)\mu_{B_i}(y) \quad i = 1, 2 \tag{8}$$

Layer-3 (average nodes): In the third layer, the nodes are labeled with *N*, demonstrating that they play a normalization

Table 3 Optimized real-time PCR protocols for quantifying nitrifiers

Real-time PCR step	Primer		
	amoA-1F/amoA-2R	FGPS872/FGPS1269	NSR1113F/NSR1264R
1. Initial activation	3:30 min at 95 °C	3:30 min at 95 °C	3:30 min at 95 °C
2. Denaturation	0:30 min at 95 °C	0:30 min at 95 °C	0:30 min at 95 °C
3. Annealing	0:30 min at 54 °C	0:30 min at 50 °C	0:30 min at 65 °C
4. Extension	0:30 min at 72 °C	0:30 min at 72 °C	0:30 min at 72 °C
5. Read fluorescence	Read	Read	Read
6. Go to step 2 for	40 times	40 times	40 times
7. Melt curve	55 to 65 °C, increment of 0.5 °C every 50 s	55 to 65 °C, increment of 0.5 °C every 50 s	55 to 65 °C, increment of 0.5 °C every 50 s
8. Read fluorescence	Read	Read	Read

Table 4 Description of qPCR standard curve parameters

Parameter	Target		
	AOB	*Nitrobacter* spp.	*Nitrospira* spp.
Efficiency (%)	102.5 ± 2.1	92.75 ± 1.63	107.3 ± 1.9
Slope	−3.3 ± 0.05	−3.5 ± 0.05	−3.2 ± 0.04
r^2 of slope	0.998 ± 0.001	0.99 ± 0.01	0.998 ± 0.04
Intercept	39.8 ± 2.2	35.0 ± 0.59	37.2 ± 0.14

role to the firing strengths from the previous layer. Thus, outputs of this layer are called "normalized firing strengths". As shown in Eq. 9, the i^{th} node calculates the ratio of the i^{th} rule's firing strength to the sum of all rules' firing strengths:

$$O_i^3 = \overline{w_i} = \frac{w_i}{w_1 + w_2} \quad i = 1,\ 2 \tag{9}$$

Layer-4 (consequent nodes): In this layer, every node i is an adaptive node with a node function. The output of each node is simply the product of the normalized firing strength and a first-order polynomial (for a first-order Sugeno model). Hence, the outputs of this layer are expressed by Eq. 10:

$$O_i^4 = \overline{w_i} f_i = \overline{w_i}(p_i x + q_i y + r_i) \quad i = 1,\ 2 \tag{10}$$

where $\overline{w_i}$ is the output of layer-3 and $\{p_i, q_i, r_i\}$ are consequent parameters, pertaining to the first-order polynomial.

Layer-5 (output node): In the fifth layer, there is only one single fixed node labeled with $\sum$. The single node computes the overall output as the summation of all incoming signals. Thus, the overall output of the model is given by Eq. 11 as follows:

$$O_i^5 = \sum_{i=1}^{2} \overline{w_i} f_i = \frac{\left(\sum_{i=1}^{2} w_i f_i\right)}{w_1 + w_2} \tag{11}$$

Application of ANFIS

The function *exhsrch* in Matlab was used to select the set of inputs that considerably impact the nitrification activity. Theoretically, *exhsrch* builds an ANFIS model for each combination and trains it for one epoch, sequentially reporting the performance achieved. ANFIS uses a hybrid learning algorithm to tune the parameters of a Sugeno-type FIS [30]. The algorithm uses a combination of the least-squares and back-propagation gradient descent methods to model a training data set [29]. The dataset is randomly classified into training (70 %) and checking (30 %) arguments. The training process stops if the designated epoch number is reached or the error goal is achieved, whichever comes first. The checking data are used for testing the generalization capability of the ANFIS and for monitoring how well the model predicts the corresponding dataset output values. Moreover, ANFIS validates models using a checking data set to test for overfitting of the training data. Recently, this technique has been successfully implemented in the field of wastewater treatment technology [17, 31].

Results and Discussion

Environmental Conditions and System Performance

Influent and effluent wastewater characteristics of the full-scale WWTP over the 237-day monitoring period are displayed in Fig. 3. Operational conditions of the treatment plant were classified into phase 1 and phase 2, corresponding to winter and summer seasons, respectively (Table 5). The temperature measurements during winter (16.5 ± 2.1 °C) and summer (22.4 ± 2.7 °C) recorded were lower than the optimum temperature range of 25–30 °C for most strains of nitrifiers [32]. The winter season (1st–78th day) experienced little or no rainfall resulting in an average influent flow rate of 61, 990 ± 2172 m^3 day^{-1}, while it increased to 93,062 ± 18,

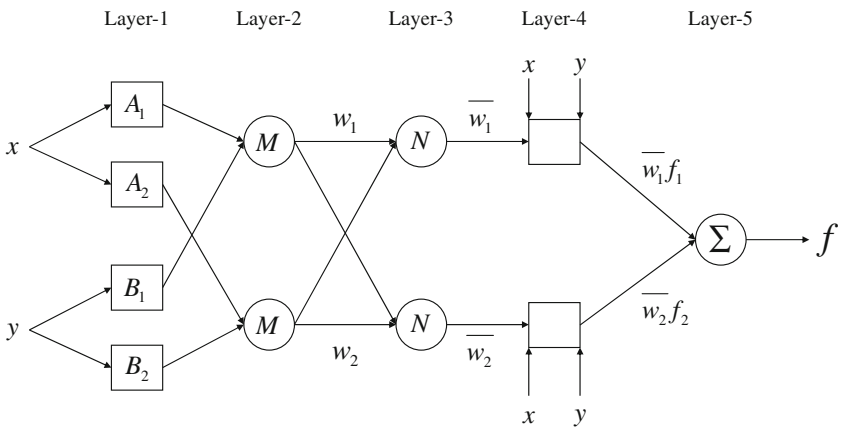

Fig. 2 Typical first-order Sugeno ANFIS architecture

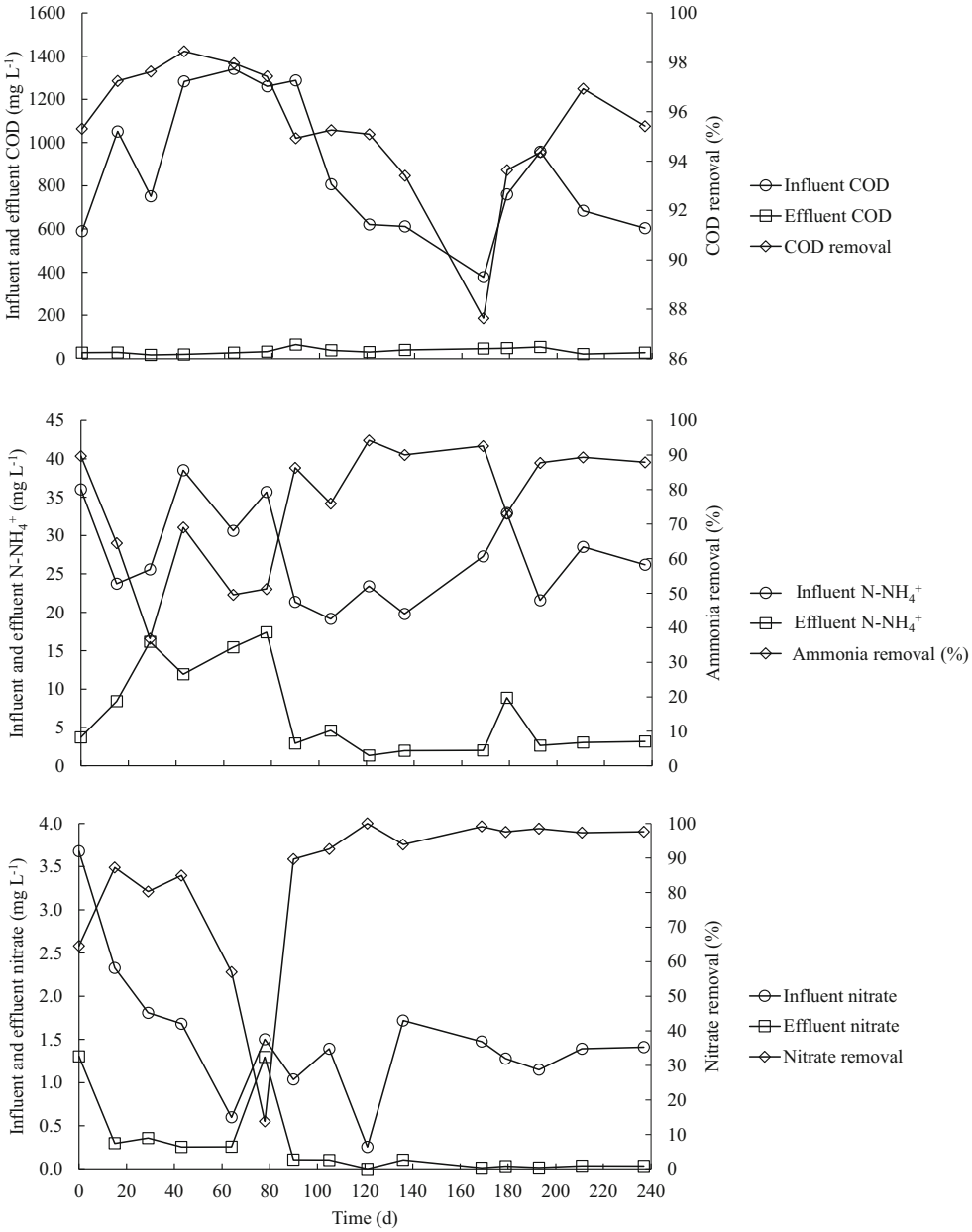

Fig. 3 Influent and effluent characteristics of the full-scale wastewater treatment plant under study

106 m^3 day^{-1} during the summer (79th–237th day). The influent COD during the summer was 1.3-fold lower than in the winter due to the dilution effect of increased rainfall. The OLR increased during summer with increasing flow rate, despite the lower COD, and reached 4.5 ± 1.8 kg COD m^{-3} day^{-1}. The deviations in OLRs could be attributed to the variation in the type of influent as a result of commercial and industrial activities occurring around the treatment plant. Under these fluctuating conditions, a steady COD removal efficiency of 95 ± 3 % was still maintained (Fig. 3). The F/M ratio was 0.6 ± 0.1 day^{-1} in the winter and increased by 48 % during the summer (Table 5). There is no ideal F/M ratio that can work for all activated sludge treatment systems. Previous studies indicate that the recommended range for F/M ratio in conventional, completely mixed, and high rate activated sludge processes ranged between 0.2–0.4, 0.2–0.6, and 0.4–1.5 day^{-1}, respectively [33].

Although the influent ammonia during summer was 1.2-fold lower than in winter, the respective ALR increased by 18.8 % resulting from the summer rainfall (Table 5). The ammonia removal efficiency improved from 60 ± 18 to 83 ± 13 % although the ALR rose from 121 ± 22 to 144 ± 29 g $N\text{-}NH_4^+$ m^{-3} day^{-1} through winter to summer, respectively. Nitrification rate followed the same trend of ammonia removal, where it also increased by 60 % and recorded 119 ± 30 g $N\text{-}NH_4^+$ m^{-3} day^{-1} during the summer season. The increase in ammonia removal efficiency and nitrification rate with ALR indicated that ammonia concentration was not the

Table 5 Operational conditions and ANFIS model parameters of the full-scale wastewater treatment plant under study

Parameters	Phase 1 (winter)	Phase 2 (summer)
Rainfall (mm)	26.0 ± 18.6	116.8 ± 32.0
Temperature (°C)	16.5 ± 2.1	22.4 ± 2.7
HRT (h)	6.3 ± 0.2	4.3 ± 1.0
OLR (kg COD m^{-3} day^{-1})	4.0 ± 1.1	4.5 ± 1.8
ALR (g N-NH_4^+ m^{-3} day^{-1})	121 ± 22	144 ± 29
F/M (g COD g^{-1} MLSS day^{-1})	0.6 ± 0.1	0.9 ± 0.3
q_N (mg N-NH_4^+ g^{-1} MLSS day^{-1})	12.3 ± 6.1	26.6 ± 10.7
AOB (copies × 10^9 L^{-1})	1.00 ± 0.86	7.35 ± 5.75
Nitrobacter spp. (copies × 10^9 L^{-1})	34.8 ± 19.0	50.8 ± 46.1
Nitrospira spp. (copies × 10^9 L^{-1})	3.32 ± 0.60	11.9 ± 11.2

HRT hydraulic retention time, *OLR* organic loading rate, *ALR* ammonia loading rate, *F/M* food to microorganisms ratio, q_N specific nitrification rate, *AOB* ammonia-oxidizing bacteria

nitrification limiting factor in this plant. This suggested that other operational conditions had higher influence on the nitrification process rather than ALR. Results from our study were lower than the 97–99.9 % ammonia removal that was obtained by Campos et al. [3] when the nitrifying activated sludge unit was subjected to high nitrogen loading rates (up to 7500 g N-NH_4^+ m^{-3} day^{-1}). The higher nitrification performance of the plant could be due to operation of the unit under a controlled environment, where the nitrifying activated sludge was fed with synthetic wastewater containing ammonia and other nutrient sources with regulated pH. The influent nitrate concentration during the study period varied between 0.25 and 3.68 mg L^{-1} with an average value of 1.51 ± 0.77 mg L^{-1} (Fig. 3). Nitrate removal efficiencies exhibited 64.6 ± 27.6 and 88.0 ± 26.3 % during winter and summer seasons, respectively. The concentration of effluent nitrate during the winter was 3.6-fold higher than summer. This might be an indication of the increased NOB/AOB ratio during the winter that promotes nitrate accumulation and thus a higher effluent nitrate concentration in winter [6, 34]

The DO levels throughout the aeration tank varied between 0.24 and 1.27 mg L^{-1}, with an average value of 0.63 ± 0.22 mg L^{-1}. The DO concentration in our study was lower than the optimum value of 1.7 mg L^{-1} for a complete nitrification process [35]. The pH in the feed over the entire sampling period was relatively stable with an average value of 7.2 ± 0.1, which is close to the optimum for nitrifiers (7.5–8.0) [35]. Ruiz et al. [35] reported that at the range of pH 6.45–8.95, as observed here, a complete nitrification to nitrate occurs, while at pH lower than 6.45 and higher than 8.95 would result in complete inhibition of nitrification.

Identification and Quantification of Dominant Nitrifiers

The betaproteobacterial AOB, *Nitrobacter* spp., and *Nitrospira* spp. were detected in abundance throughout the sampling period (Fig. 4). The AOB population abundance was quantified using the primer set targeting the ammonia monooxygenase (amoA) gene locus, whereas *Nitrobacter* and *Nitrospira* 16S rDNAs were targeted for the NOB. The specificity of the primers was confirmed by gel electrophoresis with the expected base pair length (AOB 490 bp; *Nitrobacter* spp. 386 bp; *Nitrospira* spp. 151 bp). The efficiencies of the qPCR runs were between 90 and 110 %, and the standard curves were linear over six orders of magnitude ($r^2 > 0.99$).

The AOB abundance was within the range of 1.55×10^8–1.65×10^{10} copies L^{-1} MLSS, whereas those of the *Nitrobacter* spp. and *Nitrospira* spp. were found to be in the range of 9.32×10^9–1.40×10^{11} copies L^{-1} MLSS and 2.39×10^9–3.76×10^{10} copies L^{-1} MLSS, respectively (Fig. 5). The *Nitrobacter* spp. abundance was 29-fold higher than that of AOB throughout the study period showing a clear dominance of NOB in the selected WWTP. The average AOB to NOB ratio varied from 0.03:1 (winter) to 0.15:1 (summer), which was lower than the theoretical ratio of 2:1 reported for good nitrification [36]. Due to the prevailing limiting oxygen levels (0.63 ± 0.22 mg O_2 L^{-1}) in the reactor, there was a possibility of nitrite loop. This phenomenon usually occurs when denitrifiers reduce nitrate to nitrite supplying additional nitrite for NOB, leading to a higher NOB/AOB ratio than theoretically expected [36]. Additionally, Liu [37] noted that under long-term low DO, the oxygen affinity of NOB increases

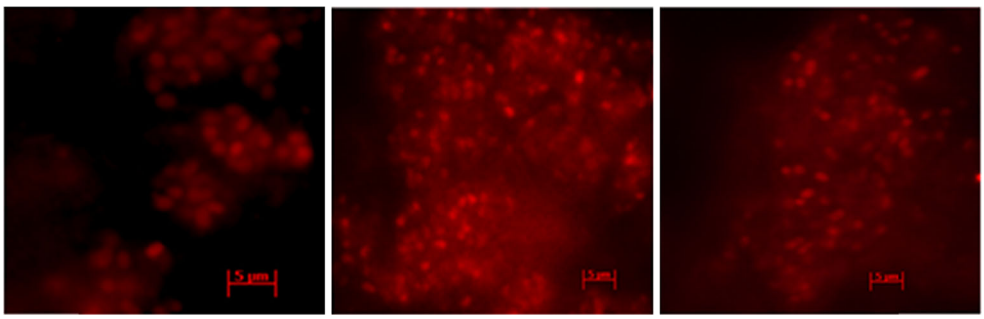

Fig. 4 Micrograph of samples hybridized with Cal 590 labeled. **a** NSO 1225 (AOB); **b** NIT3 (*Nitrobacter* spp.); **c** Ntspa 662 (*Nitrospira* spp.) oligonucleotide probes

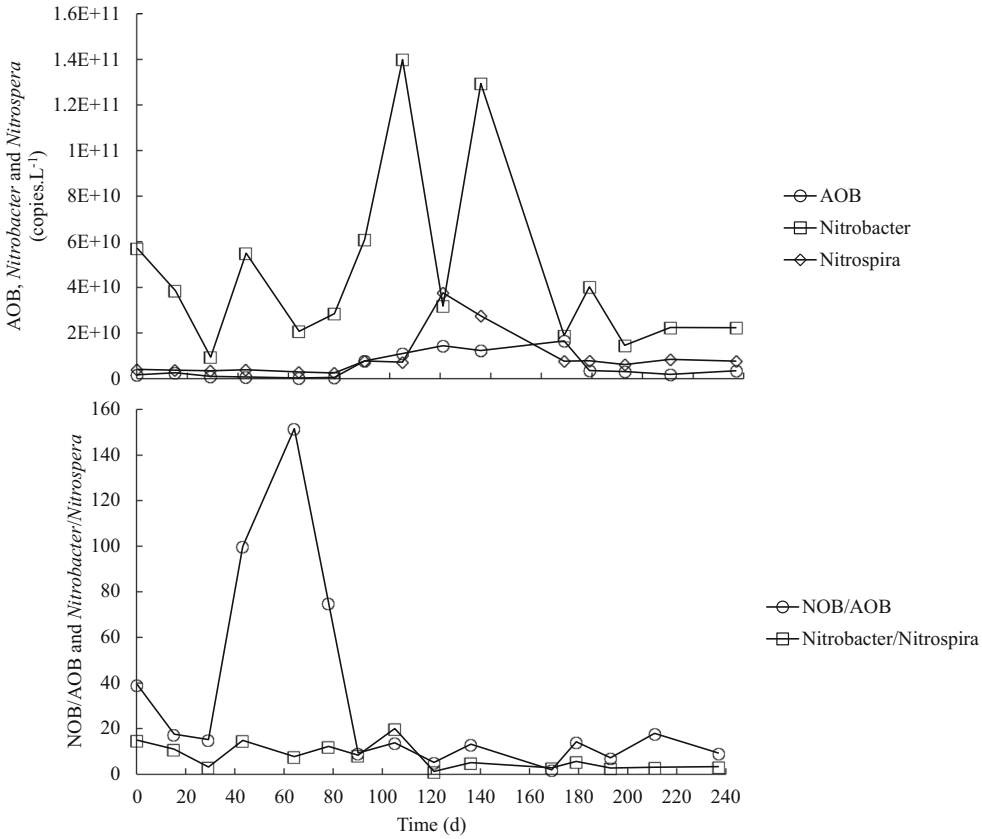

Fig. 5 Temporal changes in dominant nitrifiers of the full-scale wastewater treatment plant under study

significantly, which makes NOB a better competitor for oxygen compared to AOB. This high NOB/AOB ratio resulted in sub-optimal ammonia transformation in this study. Whereas earlier studies have recorded about 99 % ammonia removal [7], in this study the highest NH_3 removal that was recorded was 83 ± 13 %.

A higher *Nitrobacter*/*Nitrospira* ratio of 7.4: 1.0 was also recorded. This could possibly be explained based on the earlier observations of Wagner et al. [38] and Nogueira and Melo [39]. They noted an irreversible prevalence of *Nitrobacter* spp. over *Nitrospira* spp. in WWTP after a history of spike in nitrite concentration, even after subsequent reduction in nitrite concentration. *Nitrobacter* usually exhibit inhibitory effect on the growth of *Nitrospira* once it dominates. Furthermore, Fukushima et al. [40] reported that *Nitrobacter* spp. can be selected over *Nitrospira* spp. in plants with low inorganic carbon in addition to low nitrite concentration. However, there have been no studies on the distribution of *Nitrospira* and *Nitrobacter* in DO-limiting condition over an extended period of time at a full-scale WWTP. Despite several other reports that *Nitrospira* spp. often are the dominant NOB in activated sludge systems [41], the result from this study indicates that the knowledge about nitrifying bacteria populations at full-scale level still needs further investigations.

Effect of Operational Conditions on Specific Nitrification Rate

In this investigation, it was observed that the efficiency and effectiveness of a nitrifying activated sludge system depended on several factors. The specific nitrification rate (q_N) showed a strong positive correlation to temperature (r 0.726, p 0.002). The figures associated with all the regression analysis is given in Supplementary Material Figure S1, S2, S3, S4, S5, S6, and S7. The q_N noticeably increased by 2.2-fold and exhibited 26.6 ± 10.7 mg $N\text{-}NH_4^+ g^{-1}$ MLSS day^{-1} during the summer season when the temperature was elevated to 22.4 ± 2.7 °C. The ANFIS model indicated that temperature exhibited the least error, demonstrating its relevance with respect to q_N (Fig. 6a). The considerable impact of temperature on q_N could be attributed to the high seasonal variation observed during the monitored period. This observation was in agreement with previous studies, which stated that increasing temperature could enhance the rate of nitrification and nitrifier growth [42]. Xu et al. [43] reported that growth rate of nitrifiers increased exponentially at a temperature range of 10–25 °C, reaching a constant and optimal growth rate between 25 and 35 °C; however, at 40 °C the growth rate diminished drastically.

According to the ANFIS results in Fig. 6a, HRT has the second rank after temperature regarding the operational

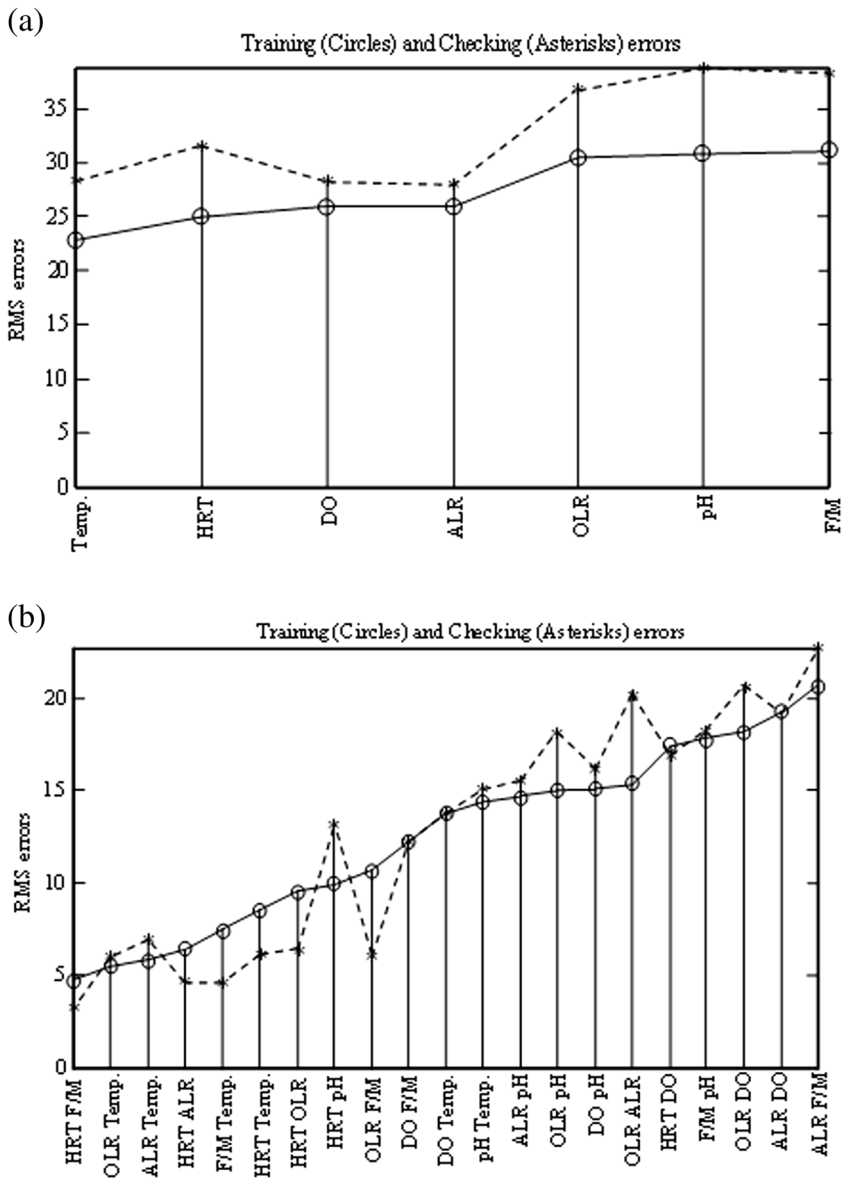

Fig. 6 Effect of operating conditions on q_N (the left-most input variable is the most relevant with respect to q_N). **a** Every input variable's influence on q_N; **b** all two-input variable combinations and their influence on q_N

conditions affecting q_N. The current study witnessed a significant increase in q_N with a decrease in HRT (r −0.651, p 0.009). This result was in agreement with a study by Li et al. [12], where q_N increased from 320 to 450 mg $N\text{-}NH_4^+$ g^{-1} MLSS day^{-1} (elevated by 41 %) when the HRT decreased from 10 to 5 h, showing that the decline in HRT led to an enhancement in ammonia oxidation activity. On the contrary, other studies have reported that lower HRT results in increasing loading rates, which negatively affects the nitrifiers due to their competition with heterotrophic bacteria for substrates (oxygen and ammonia) [44]. In our study, the negative trend between q_N and HRT can be linked to the seasonal change, which was the key factor in the development of nitrification, since q_N increased to 26.6 ± 10.7 mg $N\text{-}NH_4^+$ g^{-1} MLSS day^{-1} in summer season when temperature increased to 22.4 ± 2.7 °C, while HRT declined to 4.3 ± 1.0 h.

In the current study, q_N showed a significant positive correlation with ALR (r 0.571, p 0.026) (Supplementary Table S1, S2, S3, S4, S5, S6 and S7). However, it was found that high concentration of ammonia in the influent can negatively affect nitrification due to substrate inhibition by free ammonia [45]. This discrepancy could be attributed to the fact that the ALR of 120–140 g $N\text{-}NH_4^+$ m^{-3} day^{-1} observed in our study was still lower than the inhibitory limits reported in previous studies [3, 45]. For example, Campos et al. [3] investigated the possibilities of obtaining a full ammonia oxidation at increasing ALR from 500 to 7500 g $N\text{-}NH_4^+$ m^{-3} day^{-1}. Additionally, Kim et al.

[45] found that nitrification efficiency increased to 100 % with N-NH_4^+ loading of 700 g m^{-3} day^{-1} at 18 °C, and leachate was completely nitrified up to a load of 1500 g N-NH_4^+ m^{-3} day^{-1} at 28 °C.

Other operational conditions such as DO showed no significant effect on q_N (r −0.141, p 0.617). This observation was in agreement with a study by Kim et al. [45], who noted that DO was not a limiting factor for nitrification. Additionally, the role of pH in our study was not considerable when compared to other environmental conditions (p 0.332) due to its narrow range of variation. The pH range observed in this study (6.97–7.47) was within the optimal range for the metabolism and growth of autotrophic nitrifiers [6].

Referring to the ANFIS model (Fig. 6a), the training and checking errors were comparable, which implies that no overfitting occurred. This means that selection of more than one input can be explored to rebuild the ANFIS model. The plot in Fig. 6b showed all two-input variable combinations and their influence on q_N. It was found that HRT and F/M ratio (the left-most input variable) formed the optimal combination of two input attributes. Additionally, it was observed that the minimal training and checking errors reduced significantly from that of the best one-input model, indicating that the combination of HRT and F/M ratio improved the prediction performance. A quadratic model was developed to confirm the ANFIS results by estimating q_N over independent variables (HRT and F/M ratio). The polynomial equation (Eq. 12), including constant, linear, interaction, and squared terms, provided a determination of coefficient (r^2 value) with the experimental data of 0.50:

$$q_N = \mathrm{A} + \mathrm{B}(\mathrm{HRT}) + \mathrm{C}(\mathrm{F/M}) + D(\mathrm{HRT} \times \mathrm{F/M}) + \mathrm{E}(\mathrm{HRT})^2 + \mathrm{F}(\mathrm{F/M})^2 \quad (12)$$

A = −76.2257; B = 24.3626; C = 149.0787; D = −17.1593; E = −1.8146; F = −41.3636

where q_N is expressed in milligrams of N-NH_4^+ per gram of MLSS per day; HRT in hours; and F/M ratio in per day

Effect of Operational Conditions on AOB

The AOB was found to be HRT-dependent with an r value of −0.741 (p 0.002). The high correlation between HRT and AOB was in accordance with the ANFIS results, where HRT exhibited the least training error among other operational conditions (Fig. 7a). It was found that AOB exhibited a negative correlation with the current range of HRT (4.3–6.3 h). Similar results were reported by Li et al. [12] where an enhancement in AOB community was observed when HRT declined from 7 to 5 h. They also noted that AOB had a positive correlation when HRT became higher than 10 h [12]. Our results depicted that the AOB was considerably correlated with temperature (r 0.517 and p 0.048), indicating that temperature had a positive impact on the AOB community. The positive correlation between temperature and AOB was previously illustrated by Park et al. [46], who found that low temperature could not only decrease the attached biomass and activity of AOB but could also produce a change in the composition of the AOB species. According to ANFIS results, the two variables, HRT and temperature, were the most relevant parameters with respect to AOB (Fig. 7a). Our results suggested that an increase in AOB during the summer season resulted from an increase in temperature in line with a decrease in HRT.

As noticed from the ANFIS model (Fig. 7b), interaction of HRT with other environmental factors provided a reliable assessment of the plant performance. This might be due to the fact that the current study was based on full-scale observations where several environmental parameters were interacting together in a dynamic manner. The influence of two environmental parameters indicated that the combination of HRT and temperature exhibited lower training error than either HRT or temperature by 64 and 70 %, respectively. These results further confirm our hypothesis that the AOB increased in summer season due to the impact of both HRT and temperature.

Comparable to the q_N results, the ANFIS model indicated that the combination of HRT and F/M ratio could be the most relevant input to the AOB (output) (Fig. 7b). Subsequently, HRT and F/M ratio was employed in a polynomial function of degree 2 to determine their quadratic regression (Eq. 13). The estimated coefficient of determination showed an r^2 value of 0.614.

$$AOB = (\mathrm{A} + \mathrm{B}(\mathrm{HRT}) + \mathrm{C}(\mathrm{F/M}) + D(\mathrm{HRT} \times \mathrm{F/M}) + \mathrm{E}(\mathrm{HRT})^2 + \mathrm{F}\left(\mathrm{F}/\mathrm{M}\right)^2) \times 10^{11} \quad (13)$$

A = 1.0114; B = −0.2456; C = −0.6173; D = 0.0567; E = 0.0161; F = 0.1696

where, AOB is expressed in copies per liter; HRT in hours; and F/M ratio in per day

Effect of Operational Conditions on NOB (*Nitrobacter* and *Nitrospira*)

The presence of NOB is necessary for WWTPs to achieve complete nitrification. In this investigation, *Nitrobacter* spp. indicated no significant correlation with the operational conditions ($p > 0.1$). This suggested that the abundance of *Nitrobacter* could tolerate seasonal and environmental variations. The ANFIS model indicated that the F/M ratio had the highest impact on *Nitrobacter* abundance (Fig. 8a). The strength of the relationship between the F/M ratio and *Nitrobacter* spp. was further estimated by Pearson correlation

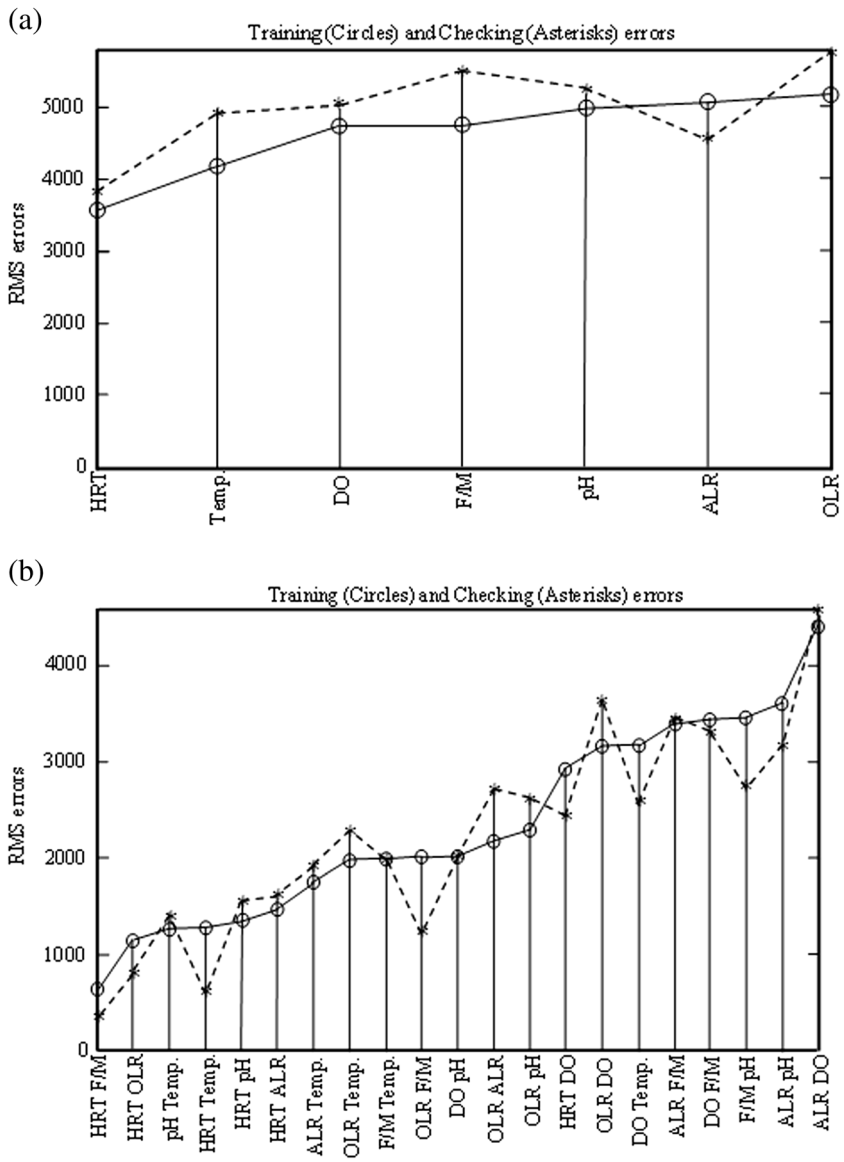

Fig. 7 Effect of operating conditions on AOB (the left-most input variable is the most relevant with respect to AOB). **a** Every input variable's influence on AOB; **b** all two-input variable combinations and their influence on AOB

coefficient which showed an r value of 0.359 ($p > 0.1$). The prominence of F/M ratio was previously reported, where some organic compounds in the wastewater positively affected the activity of NOB [45]. The ANFIS model was also used to identify relationships between *Nitrobacter* spp. abundance and the combination of two operational parameters (Fig. 8b). The model indicated that F/M ratio and temperature form the optimal combination of two input attributes. The polynomial equation of their quadratic interaction is presented in Eq. 14 (r^2 value 0.49):

$$Nitrobacter = \left(\mathrm{A} + \mathrm{B(F/M)} + \mathrm{C(T)} + D(\mathrm{F/M} \times \mathrm{T}) + \mathrm{E(F/M)}^2 + \mathrm{F(T)}^2\right) \times 10^{11} \quad (14)$$

A = −0.7143; B = −3.4550; C = 0.2579; D = −0.0050; E = 1.9650; F = −0.0062

where *Nitrobacter* is expressed in copies per liter; F/M ratio in per day; and T in degree Celsius.

Cross-correlation coefficients indicated that increase in *Nitrospira* spp. was significantly affected by a decline in HRT (r −0.627 and p 0.012). Similarly, the ANFIS model showed that the input HRT exhibited the least training error (Fig. 9a), which was in accordance with the p values. Additionally, HRT showed inverse correlation with *Nitrobacter* spp. (r −0.364 and $p > 0.1$). Similarly, Li et al. [12] reported that a short HRT favored the relative growth of

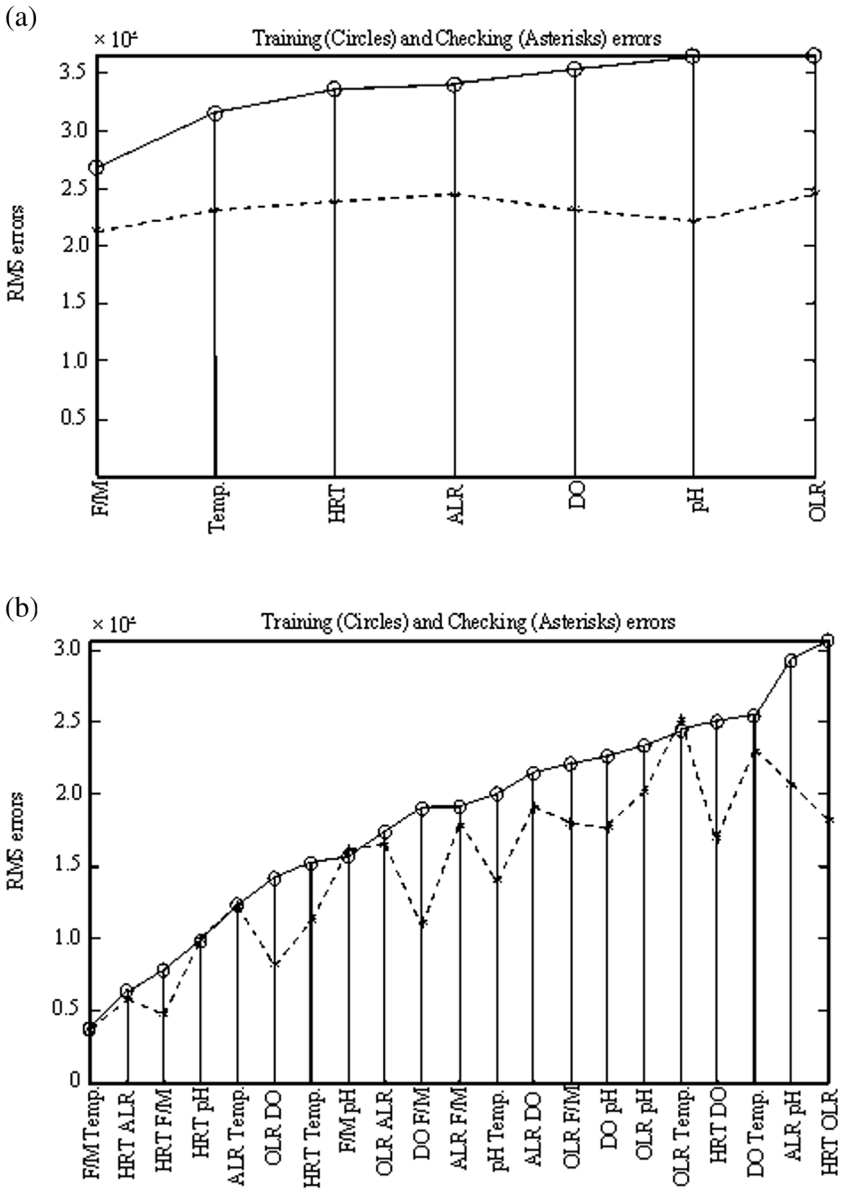

Fig. 8 Effect of operating conditions on *Nitrobacter* (the left-most input variable is the most relevant with respect to *Nitrobacter*). **a** Every input variable's influence on *Nitrobacter*; **b** all two-input variable combinations and their influence on *Nitrobacter*

NOBs, particularly the fast-growing *Nitrobacter* spp., in the conventional activated sludge system. As observed from the ANFIS results (Fig. 9b), the combination of HRT and F/M ratio exhibited a 4-fold lowering of the training error when compared to HRT individually. Therefore, the quadratic polynomial formula indicating the combinatory effect of HRT and F/M ratio on *Nitrospira* can be presented by Eq. 15 (r^2 value 0.716):

$$Nitrospira = \left(A + B(HRT) + C(F/M) + D\left(HRT \times F\Big/M\right) + E(HRT)^2 + F\left(F\Big/M\right)^2\right) \times 10^{11} \quad (15)$$

A = 1.9980; B = −0.7133; C = 0.1599; D = −0.0062; E = 0.0636; F = −0.1640

where *Nitrospira* is expressed in copies per liter; HRT in hours; and F/M ratio in per day

In a similar study, Huang, Gedalanga, and Olson [10] investigated the impact of environmental variables on *Nitrobacter* and *Nitrospira*. They observed that *Nitrobacter* populations were negatively correlated to temperature (*r*

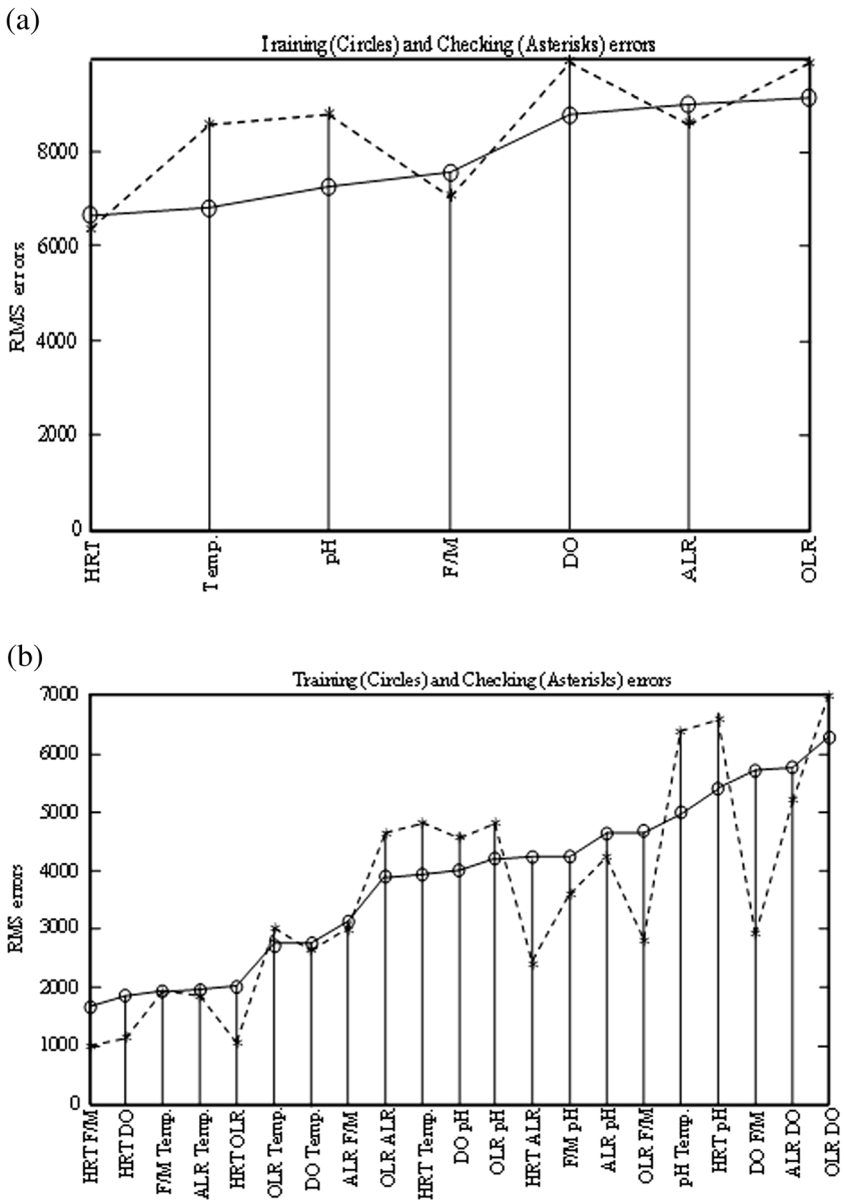

Fig. 9 Effect of operating conditions on *Nitrospira* (the left-most input variable is the most relevant with respect to *Nitrospira*). **a** Every input variable's influence on *Nitrospira*; **b** all two-input variable combinations and their influence on *Nitrospira*

−0.49 and $p < 0.001$), while the *Nitrospira* abundance showed a strong positive correlation to temperature (r 0.59 and $p < 0.0001$). Additionally, *Nitrobacter* populations were significantly and positively correlated to DO (r 0.38 and $p < 0.01$). However, *Nitrospira* abundance showed a significantly negative correlation to DO (r −0.46 and $p < 0.01$). Moreover, HRT showed a significant impact on *Nitrobacter* spp. (r 0.334 and $p < 0.05$). When comparing our study with the latter investigation [10], both studies used the cross-correlation coefficients to determine the significant impact of operational parameters on *Nitrobacter* and *Nitrospira*. However, our study further applied artificial modeling technique in confirming the r results and in determining the optimum combination of two input variables.

Conclusions

The AI approach succeeded in describing the effect of operating condition on nitrification process. Results from the ANFIS model were in accordance with Spearman's correlation coefficients, and it was concluded that:

- The *Nitrobacter* spp. abundance was 29-fold higher than that of AOB throughout the study period, showing a clear dominance of NOB.
- The q_N was noticeably increased by 2.2-fold and exhibited 26.6 ± 10.7 mg $N\text{-}NH_4^+ g^{-1}$ MLSS day^{-1} when the temperature elevated from 16.5 ± 2.1 to 22.4 ± 2.7 °C (r 0.726, p 0.002).

- The q_N was also significantly affected by HRT (r −0.651, p 0.009) and ALR (r 0.571, p 0.026).
- HRT and F/M ratio formed the optimal combination of two inputs affecting the q_N, and their quadratic equation showed an r^2 value of 0.50.
- AOB increased in the summer season, when temperature was 1.4-fold higher than during winter (r 0.517, p 0.048), and HRT decreased by 31 % as a result of rainfall (r −0.741, p 0.002).
- No single input has a significant effect on *Nitrobacter* spp., indicating that the abundance of *Nitrobacter* could tolerate seasonal and environmental variations.
- *Nitrospira* spp. increased by 3.6 times when HRT declined during the summer season (r −0.627, p 0.012).
- A polynomial function of 2nd degree for HRT, F/M ratio, and AOB; F/M ratio, temperature, and *Nitrobacter*; and HRT, F/M ratio, and *Nitrospira* showed r^2 values of 0.61, 0.49, and 0.72, respectively.

Acknowledgments The authors hereby acknowledge the Durban University of Technology and National Research Foundation for providing financial assistance.

References

1. Kim YM, Cho HU, Lee DS, Park D, Park JM (2011) Influence of operational parameters on nitrogen removal efficiency and microbial communities in a full-scale activated sludge process. Water Res 45:5785–5795. doi:10.1016/j.watres.2011.08.063
2. Angel R, Asaf L, Ronen Z, Nejidat A (2010) Nitrogen transformations and diversity of ammonia-oxidizing bacteria in a desert ephemeral stream receiving untreated wastewater. Microb Ecol 59:46–58
3. Campos J, Garrido-Fermindez J, Mendez R, Lema J (1999) Nitrification at high ammonia loading rates in an activated sludge unit. Bioresour Technol 68:141–148
4. Nasr M, Moustafa M, Seif H, El Kobrosy G (2011) Modelling and simulation of German BIOGEST/EL-AGAMY wastewater treatment plants—Egypt using GPS-X simulator. Alexandria Eng J 50:351–357
5. Third K, Paxman J, Schmid M, Strous M, Jetten M, Cord-Ruwisch R (2005) Enrichment of anammox from activated sludge and its application in the CANON process. Microb Ecol 49:236–244
6. Zhang L, Jiang J, Yang J, Hira D, Furukawa K (2012) High rate nitrogen removal by the CANON process at ambient temperature. Water Sci Technol : J Int Assoc Water Pollut Res 65:1826–1833
7. Hu J, Li D, Liu Q, Tao Y, He X, Wang X, Li X, Gao P (2009) Effect of organic carbon on nitrification efficiency and community composition of nitrifying biofilm. J Environ Sci 21:387–394. doi:10.1016/S1001-0742(08)62281-0
8. Fulweiler RW, Emery HE, Heis EM, Berounsky VM (2011) Assessing the role of pH in determining water column nitrification rates in a coastal system. Estuar Coasts 34:1095–1102
9. Stark J (1996) Modeling the temperature response of nitrification. Biogeochemistry 35:433–445
10. Huang H, Gedalanga P, Olson BH (2010) Distribution of nitrobacter and nitrospira communities in an aerobic activated sludge bioreactor and their contributions to nitrite oxidation. WEFTEC
11. Wu YJ, Whang LM, Chang MY, Fukushima T, Lee YC, Cheng SS, Hsu SF, Chang CH, Shen W, Yang CY, Fu R, Tsai TY (2013) Impact of food to microorganism (F/M) ratio and colloidal chemical oxygen demand on nitrification performance of a full-scale membrane bioreactor treating thin film transistor liquid crystal display wastewater. Bioresour Technol 141:35–40. doi:10.1016/j.biortech.2013.02.108
12. Li H, Zhang Y, Yang M, Kamagata Y (2013) Effects of hydraulic retention time on nitrification activities and population dynamics of a conventional activated sludge system. Front Environ Sci Eng China 7:43–48. doi:10.1007/s11783-012-0397-8
13. Klemetti R (2010) Modelling the start-up of biological phosphorus removal at low temperature. Aato University
14. Nasr M, Mahmoud AED, Fawzy M, Radwan A (2015) Artificial intelligence modeling of cadmium(II) biosorption using rice straw. Appl Water Sci. doi:10.1007/s13201-015-0295x
15. Nasr M, Moustafa M, Seif H, El Kobrosy G (2012) Application of artificial neural network (ANN) for the prediction of EL-AGAMY wastewater treatment plant performance-EGYPT. Alexandria Eng J 51:37–43
16. Nasr M, Moustafa M, Seif H, El-Kobrosy G (2014) Application of fuzzy logic control for Benchmark simulation model.1. Sustain Environ Res 24:235–243
17. Nasr M, Ateia M, Hassan K (2015) Artificial intelligence for greywater treatment using electrocoagulation process. Sep Sci Technol. doi:10.1080/01496395.2015.1062399
18. Daims H, Wagner M (2010) The microbiology of nitrogen removal. In: Seviour RJ, Nielsen PH (eds) Microbial ecology of activated sludge. IWA, London, pp 259–280
19. Fuchs BM, Pernthaler J, Amann R (2007) Single cell identification by fluorescence in situ hybridization. In: Reddy CA, Beveridge TJ, Breznak JA, Marzluf G, Schmidt TM, Snyder LR (eds) Methods for general and molecular microbiology, 3rd edn. ASM Press, Washington D.C., pp 886–896
20. Nielsen JL (2009) Protocol for fluorescence in situ hybridization (FISH) with rRNA-targeted oligonucleotides. In: Nielsen PH, Daims H, Lemmer H (eds) FISH handbook for biological wastewater treatment. IWA Publishing, London, pp 73–84
21. Bassin JP, Kleerebezem R, Muyzer G, Rosado AS, van Loosdrecht MC, Dezotti M (2012) Effect of different salt adaptation strategies on the microbial diversity, activity, and settling of nitrifying sludge in sequencing batch reactors. Appl Microbiol Biotechnol 93:1281–1294. doi:10.1007/s00253-011-3428-7
22. Wu P, JI X, Song X, Shen Y (2014) Mechanism of efficient nutrient removal and microbial analysis of a combined anaerobic baffled reactor–membrane bioreactor process. Int J Environ Sci Technol 11:1611–1618
23. Purkhold U, Pommerening-Röser A, Juretschko S, Schmid MC, Koops HP, Wagner M (2000) Phylogeny of all recognized species of ammonia oxidizers based on comparative 16S rRNA and amoA sequence analysis: implications for molecular diversity surveys. Appl Environ Microbiol 66:5368–5382
24. Lienen T, Kleybocker A, Verstraete W, Wurdemann H (2014) Moderate temperature increase leads to disintegration of floating sludge and lower abundance of the filamentous bacterium *Microthrix parvicella* in anaerobic digesters. Water Res 65:203–212. doi:10.1016/j.watres.2014.07.019
25. Geets J, de Cooman M, Wittebolle L, Heylen K, Vanparys B, De Vos P, Verstraete W, Boon N (2007) Real-time PCR assay for the simultaneous quantification of nitrifying and denitrifying bacteria in activated sludge. Appl Microbiol Biotechnol 75:211–221. doi:10.1007/s00253-006-0805-8
26. Steinberg LM, Regan JM (2009) mcrA-targeted real-time quantitative PCR method to examine methanogen communities. Appl Environ Microbiol 75:4435–4442. doi:10.1128/AEM.02858-08

27. APHA (1998) Standard Methods for the Examination of Water and Wastewater American Public Health Association
28. Tchobanoglous G, Burton FL, Stensel HD (2003) Wastewater engineering: treatment and reuse. Metcalf and Eddy Inc. McGraw-Hill, New York
29. Jang JS (1993) ANFIS: adaptive-Network-based Fuzzy Inference Systems. IEEE Trans Syst Man Cybern 23:665–685
30. Azar A (2011) Adaptive neuro-fuzzy system as a novel approach for predicting post-dialysis urea rebound. Int J Intell Syst Technol Appl 10:302–330
31. Fawzy M, Nasr M, Abdel-Gaber A, Fadly S (2015) Biosorption of Cr(VI) from aqueous solution using agricultural wastes, with artificial intelligence approach. Sep Sci Technol. doi:10.1080/01496395.2015.1115068
32. Watson S, Valois F, Waterbury J (1981) The family Nitrobacteraceae. In: Starr MP, Stolp H, Truper HG, Balows A, Schlegel HG (eds) The prokaryotes. Springer, Berlin, pp 1005–1022
33. Tchobanoglous G, Burton F (1991) Wastewater engineering treatment, disposal and reuse. McGraw-Hill, New York
34. Mozumder MS, Picioreanu C, van Loosdrecht MC, Volcke EI (2013) Effect of heterotrophic growth on autotrophic nitrogen removal in a granular sludge reactor. Environ Technol 35:1027–1037
35. Ruiz G, Jeison D, Chamy R (2003) Nitrification with high nitrite accumulation for the treatment of wastewater with high ammonia concentration. Water Res 37:1371–1377
36. Winkler MK, Bassin JP, Kleerebezem R, Sorokin DY, van Loosdrecht MC (2012) Unravelling the reasons for disproportion in the ratio of AOB and NOB in aerobic granular sludge. Appl Microbiol Biotechnol 94:1657–1666. doi:10.1007/s00253-012-4126-9
37. Liu G (2012) Nitrification performance of activated sludge under low dissolved oxygen conditions. PhD, Missouri University of Science and Technology
38. Wagner M, Loy A, Nogueira R, Purkhold U, Lee N, Daims H (2002) Microbial community composition and function in wastewater treatment plants. Antonie Van Leeuwenhoek 81:665–680
39. Nogueira R, Melo LF (2006) Competition between *Nitrospira* spp. and *Nitrobacter* spp. in nitrite-oxidizing bioreactors. Biotechnol Bioeng 95:169–175. doi:10.1002/bit.21004
40. Fukushima T, Whang LM, Chiang TY, Lin YH, Chevalier LR, Chen MC, Wu YJ (2013) Nitrifying bacterial community structures and their nitrification performance under sufficient and limited inorganic carbon conditions. Appl Microbiol Biotechnol 97:6513–6523. doi:10.1007/s00253-012-4436-y
41. Whang LM, Chien IC, Yuan SL, Wu YJ (2009) Nitrifying community structures and nitrification performance of full-scale municipal and swine wastewater treatment plants. Chemosphere 75:234–242
42. Tarre S, Green M (2004) High-rate nitrification at low pH in suspended and attached biomass reactors. Appl Environ Microbiol 70:6481–6487
43. Xu M, Schnorr J, Keibler B, Simon HM (2012) Comparative analysis of 16S rRNA and amoA genes from archaea selected with organic and inorganic amendments in enrichment culture. Appl Environ Microbiol 78:2137–2146. doi:10.1128/AEM.06845-11
44. Nogueira R, Melo L, Purkhold U, Wuertz S, Wagner M (2002) Nitrifying and heterotrophic population dynamics in biofilm reactors: effects of hydraulic retention time and the presence of organic carbon. Water Res 36:469–481
45. Kim D, Lee D, Keller J (2006) Effect of temperature and free ammonia on nitrification and nitrite accumulation in landfill leachate and analysis of its nitrifying bacterial community by FISH. Bioresour Technol 97:459–468
46. Park J, Byun I, Park S, Park D (2008) Nitrifying bacterial communities and its activities in aerobic biofilm reactors under different temperature conditions. Korean J Chem Eng 25:1448–1455